AGU PUBLICATIONS

Geophysical Research Letters

RESEARCH LETTER
10.1002/2016GL071841

Key Points:
- We identify evidence for new gas hydrate accumulations in the SW Barents Sea
- We model future hydrate dissociation scenario incorporating structure II hydrates
- Up to 8 Gt of carbon released into the SW Barents Sea water column in the period 1960–2060

Supporting Information:
- Supporting Information S1

Correspondence to:
S. Vadakkepuliyambatta,
sunil.vadakkepuliyambatta@uit.no

Citation:
Vadakkepuliyambatta, S., S. Chand, and S. Bünz (2017), The history and future trends of ocean warming-induced gas hydrate dissociation in the SW Barents Sea, *Geophys. Res. Lett.*, *44*, doi:10.1002/2016GL071841.

Received 5 NOV 2016
Accepted 11 JAN 2017
Accepted article online 13 JAN 2017

©2017. American Geophysical Union. All Rights Reserved.

The history and future trends of ocean warming-induced gas hydrate dissociation in the SW Barents Sea

Sunil Vadakkepuliyambatta[1], Shyam Chand[1,2], and Stefan Bünz[1]

[1]Centre for Arctic Gas Hydrate, Environment and Climate, Department of Geosciences, UiT-The Arctic University of Norway, Tromsø, Norway, [2]Geological Survey of Norway (NGU), Trondheim, Norway

Abstract The Barents Sea is a major part of the Arctic where the Gulf Stream mixes with the cold Arctic waters. Late Cenozoic uplift and glacial erosion have resulted in hydrocarbon leakage from reservoirs, evolution of fluid flow systems, shallow gas accumulations, and hydrate formation throughout the Barents Sea. Here we integrate seismic data observations of gas hydrate accumulations along with gas hydrate stability modeling to analyze the impact of warming ocean waters in the recent past and future (1960–2060). Seismic observations of bottom-simulating reflectors (BSRs) indicate significant thermogenic gas input into the hydrate stability zone throughout the SW Barents Sea. The distribution of BSR is controlled primarily by fluid flow focusing features, such as gas chimneys and faults. Warming ocean bottom temperatures over the recent past and in future (1960–2060) can result in hydrate dissociation over an area covering 0.03–38% of the SW Barents Sea.

1. Introduction

Gas hydrates, solid compounds of water and gas, have gained significant attention due to both their potential as a future energy resource and as a hazard to the environment. Sediments containing gas hydrates are found within specific pressure-temperature conditions in permafrost regions and abundantly beneath the seabed in continental margins [*Kvenvolden*, 1988]. Methane is the most abundant gas in naturally occurring gas hydrates [*Kvenvolden and McMenamin*, 1980]. Dissociation of gas hydrates, resulting from changes in stability conditions, and subsequent release of greenhouse gases have the potential to enhance global warming and contribute to submarine landslides [*Bugge et al*., 1987; *Kennett et al*., 2003; *Maslin et al*., 2010]. Gas hydrates in polar regions may be particularly sensitive to environmental variations as climate changes are felt here first and may be more severe than elsewhere [*Marín-Moreno et al*., 2013; *Fetterer et al*., 2016].

The stability of gas hydrates in sediments is primarily affected by changes in bottom water temperature (BWT), geothermal gradient, seabed pressure, composition of the gas, and pore water salinity [*Sloan*, 1990]. These parameters define the region where hydrates can be stable, generally known as the gas hydrate stability zone (GHSZ). In marine sediments, the presence of gas hydrates can be inferred from an observation of bottom-simulating reflectors (BSRs) in the seismic data [*Shipley et al*., 1979]. The BSR represents the base of the GHSZ and originates from a large acoustic impedance contrast between overlying sediments containing hydrates and the underlying zone of free gas that accumulates beneath the hydrates. The BSR is normally characterized by high amplitudes and reversed polarity with respect to the seafloor reflection. It often mimics the seafloor and, therefore, may crosscut other sedimentary reflections.

The SW Barents Sea is a large petroleum province in the Norwegian Arctic region (Figure 1a), where warm waters from the northern limb of the Gulf Stream mixes with frigid Arctic waters. The Barents Sea was affected by multiple periods of glaciations and associated glaciotectonic and erosional processes during the Cenozoic, which led to leakage of hydrocarbons from deeper reservoirs [*Doré and Jensen*, 1996; *Henriksen et al*., 2011]. Those hydrocarbons mostly accumulated in the shallow subsurface forming shallow gas accumulations and gas hydrates [*Chand et al*., 2012; *Ostanin et al*., 2012; *Vadakkepuliyambatta et al*., 2013]. The Barents Sea constitutes the largest shallow shelf sea in the Arctic with a vast area where gas hydrates might occur at the upper edge of stability.

Gas hydrate stability in the SW Barents Sea is highly variable, and the presence of higher-order hydrocarbons, heat flow, and salt tectonics could be some of the major factors controlling stability conditions [*Chand et al*., 2008]. However, considering the complex structural setting of the sedimentary basins in the SW Barents Sea and the highly variable GHSZ, more constraints on the stability parameters are

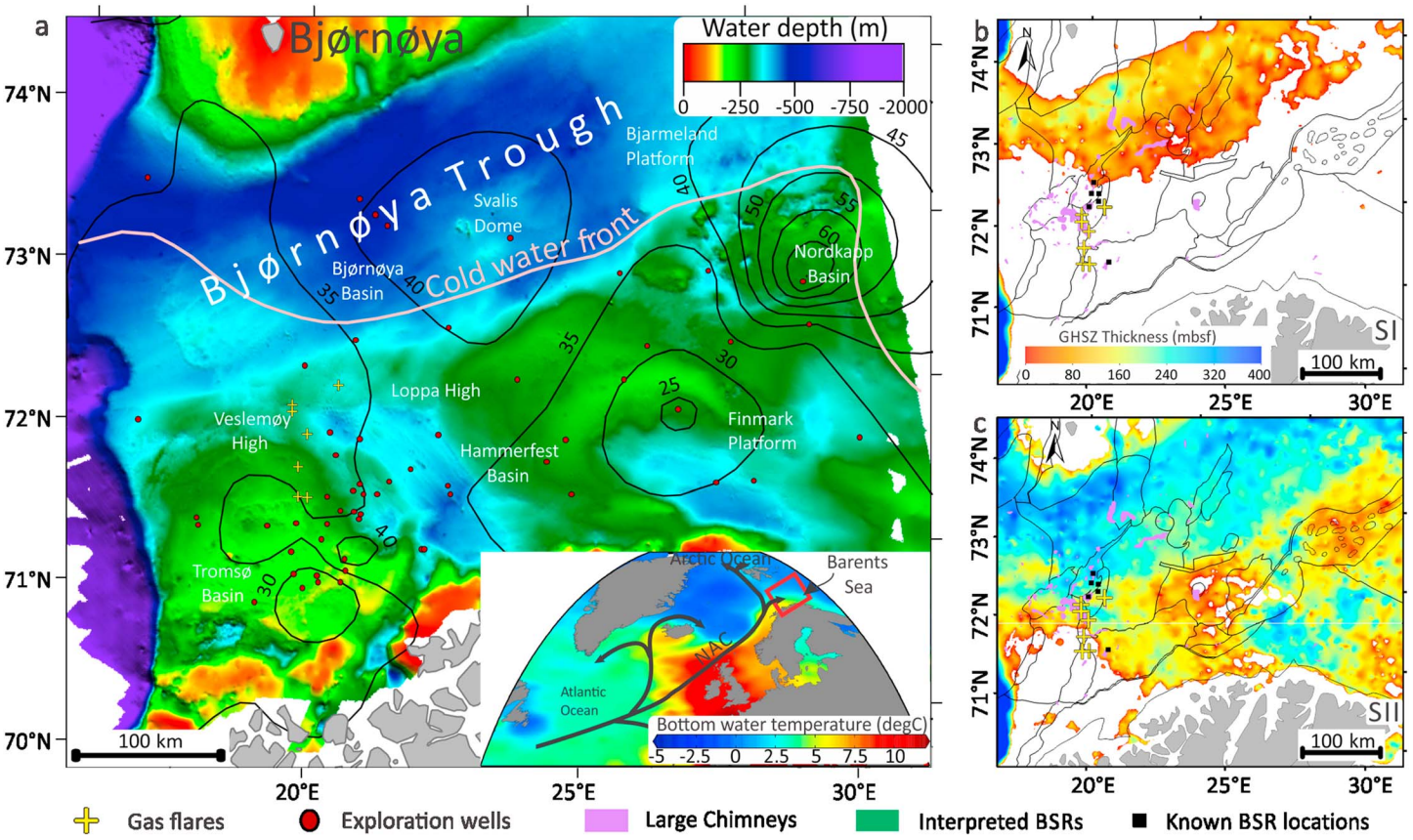

Figure 1. (a) General bathymetry of SW Barents Sea along with exploration well locations, known gas seeps [*Chand et al.*, 2012], and geothermal gradients from wells (black contours) [*Bugge et al.*, 2002]. Inset figure shows the present bottom water temperatures in the North Atlantic and the location of the study area. NAC, North Atlantic Current. Modeled gas hydrate stability thickness in the SW Barents Sea. (b) SI (100% methane). (c) SII (96% methane + 3% ethane + 1% propane).

necessary for a better understanding of hydrate stability. In addition, recent warming of ocean bottom temperatures (up to 1°C in the last 50 years) may have influenced gas hydrate stability [*Westbrook et al.*, 2009; *Ferré et al.*, 2012]. The intermixing of warm and cold water as well as their seasonal and long-term variations may cause the depletion of the gas hydrate reservoirs and subsequent release of greenhouse gases into the ocean. Situated at the northern limb of the Gulf Stream, the SW Barents Sea might thus be by far the most extensive and most sensitive gas hydrate system in the Arctic, if not worldwide. Here we employ an integrated analysis of transient hydrate stability modeling and 2-D seismic data to document the distribution of hydrate accumulations in the SW Barents Sea and the impact of warming ocean bottom waters on hydrate stability over the period 1960–2060.

2. Gas Hydrates in the Barents Sea

Gas hydrates are inferred from BSR in many parts of the SW Barents Sea [*Andreassen et al.*, 1990; *Løvø et al.*, 1990; *Laberg and Andreassen*, 1996; *Chand et al.*, 2012; *Ostanin et al.*, 2013] (Figures 1b and 1c). Most of these gas hydrate accumulations are associated with gas chimneys and shallow gas accumulations resulting from spillage of hydrocarbons through faults and fractures [*Laberg et al.*, 1998; *Ostanin et al.*, 2013; *Vadakkepuliyambatta et al.*, 2013]. Observations of deeper BSR in the seismic data from the SW Barents Sea suggest contribution of higher-order thermogenic gases [*Laberg et al.*, 1998; *Ostanin et al.*, 2013], and such gas hydrates could be stable in most parts of the SW Barents Sea [*Chand et al.*, 2008]. Among the various parameters controlling the GHSZ, only BWT is relatively well constrained in the SW Barents Sea [*National Oceanographic Data Center* (*NODC*), 2013]. Since very few heat flow measurements exist in the SW Barents Sea [*Bugge et al.*, 2002; *Cavanagh et al.*, 2006; *Pascal*, 2015], we use bottomhole temperature

measurements from exploration well data to constrain geothermal gradients. Gas sample analyses from the area are also rare, and we utilize gas sample analyses from deep exploration wells to model site-specific gas hydrate stability thicknesses.

3. Methodology

3.1. Steady State and Transient Gas Hydrate Stability Modeling

The GHSZ for the whole SW Barents Sea is estimated using the CSMHYD program [*Sloan and Koh*, 2008] (See supporting information Text S4), using IBCAOv3 bathymetry [*Jakobsson et al*., 2012], assuming a pore water salinity of 35‰, and considering variations in BWT for the period 1960–2060. The BWT in the SW Barents Sea can vary up to 2.5°C seasonally (generally, less than 1°C) [*NODC*, 2013]. However, it is highly unlikely that these variations could affect hydrates located more than few tens of meters below seafloor. At similar water depths in the West Svalbard region, the seasonal temperature variation is found to affect hydrates within top 5 m of surface sediments [*Berndt et al*., 2014]. In view of this, we use a yearly averaged observed BWTs for the period 1960–2010 [*NODC*, 2013], whereas a linear increase of 1°C [*Ferré et al*., 2012] is used for the period 2010–2060. The diffusive transport of heat through the sediments is estimated using a 3-D finite difference heat flow model and sediment properties appropriated from well data close to Hammerfest Basin [*Woodside and Messmer*, 1961; *Brady and Weil*, 1996; *Laberg et al*., 1998; *Waples and Waples*, 2004; *Duran et al*., 2013]. More details on the heat flow modeling can be found in the supporting information (supporting information Text S3) [*Turcotte and Schubert*, 2002; *Spiegelman*, 2004; *Gerya*, 2010; *Phrampus and Hornbach*, 2012]. A new thermal gradient map is generated for the SW Barents Sea using corrected temperature measurements from deep boreholes [*Peters and Nelson*, 2009] (See supporting information Text S1) and published data [*Bugge et al*., 2002] (See supporting information Text S2 and Figure S2.3), which range from 22.8 to 69.3°C/km. The higher geothermal gradients are observed close to salt domes in the Nordkapp Basin. The average geothermal gradient in the SW Barents Sea is 36°C/km. In addition to biogenic gas contributing to the formation of hydrates, thermogenic gas is suspected to be a major contributor to shallow gas, since fluid flow from deeper source rocks is widespread in the area [*Vadakkepuliyambatta et al*., 2013]. Consequently, we consider two different gas compositions for the regional hydrate stability modeling in the study area (SI: 100% methane and SII: 96% methane + 3% ethane + 1% propane). In addition, site-specific GHSZ depths at borehole locations are calculated using gas analysis data from individual wells (See supporting information Text S2 and Figure S2.4) in order to further support identification of BSR in seismic data.

3.2. Identification of BSR in the Seismic Data

About 3000 industry 2-D multichannel seismic profiles (See supporting information Text S1) were used to identify potential gas hydrate accumulations in the study area using mostly the BSR as the major indicator for the presence of gas hydrates. The 2-D seismic data are from different surveys with varying data quality and resolutions acquired over several decades and processed by hydrocarbon and geophysical service industry. The gas hydrate stability models (both regional and site specific) facilitated a much-improved identification of gas hydrates and their distinction from abundant shallow gas accumulations.

4. Results and Discussion

4.1. Present-Day Gas Hydrate Stability Zone in the SW Barents Sea

The gas hydrate stability modeling for steady state conditions shows a highly variable GHSZ in the SW Barents Sea, influenced primarily by heat flow and BWT conforming to previous studies [*Chand et al*., 2008]. Pure methane hydrates (SI) are stable, generally up to 150 m below the seafloor (mbsf), mainly in the Bjørnøya Trough region (Figure 1b). Hydrates with SII composition show much wider range of stability and can occur up to ~400 mbsf (Figure 1c). The geothermal gradient has a major influence on GHSZ thickness in few areas such as Nordkapp Basin (due to presence of salt domes) and Finnmark Platform (low geothermal gradients may be contributing to thicker GHSZ) (Figures 1b and 1c). BWT plays a major role in the Tromsø Basin and Bjørnøya Basin (Figures 1b and 1c). High BWTs (~6°C) and shallow water depth make gas hydrates unstable in the Tromsø Basin (Figure 1b and supporting information Text S2.1), whereas relatively low BWTs (~2°C) (and deeper water depth) in the Bjørnøya Basin provide suitable stability conditions for SI hydrates. Gas composition seems to be another factor affecting hydrate stability and GHSZ thickness irrespective of the basin structure and oceanographic conditions. The available gas composition data from exploration wells suggest

very high local variability (Figure S2.3). Most of the previously observed BSR fall outside the GHSZ of SI hydrates, suggesting a predominant thermogenic input to the GHSZ in the SW Barents Sea (Figures 1b and 1c).

Our improved GHSZ modeling in the SW Barents Sea shows a much shallower (up to ~400 m) GHSZ thickness than previously estimated. *Chand et al.* [2008], assuming a geothermal gradient of 22.8°C/km and SII composition, calculated a maximum possible GHSZ thickness of 800 mbsf in the Bjørnøya Trough. Although such lower geothermal gradients are present in the Nordkapp Basin, bottomhole temperature measurements from the Bjørnøya Trough show generally higher thermal gradients (>38°C/km). Nonetheless, gas composition can play a major role in increasing the GHSZ thickness. Given the variability of gas composition in the SW Barents Sea (Figure S2.3), higher GHSZ thickness (>400 m) is conceivable.

4.2. Bottom-Simulating Reflectors in the Seismic Data

Interpretation of multichannel 2-D seismic profiles covering the whole SW Barents Sea shows numerous high-amplitude anomalies indicating shallow gas accumulations. Some of these accumulations fall close to the modeled GHSZ and exhibit seismic characteristics of a gas hydrate-related BSR (reverse polarity reflections and crosscutting the surrounding lithology) and are interpreted as such (e.g., Figures 2a and 2b). Among the interpreted BSR, the majority lie close to the modeled base of GHSZ using gas composition SII (Figures 2b and 2d) hinting at a mostly thermogenic gas source. In addition, gas compositions from the borehole data (See supporting information Text S2) show presence of higher-order hydrocarbons in most locations. Some of the reflections were patchy and lie deeper than the modeled base of GHSZ for SII composition (Figure 2 a), suggesting higher concentrations of higher-order hydrocarbons than assumed. Apart from the high-amplitude reflections indicating accumulation of shallow gas, vertical zones of weak, disturbed seismic signals were also observed (Figure 2b). Such regions of highly disrupted seismic signals may indicate upward fluid flow and can be termed as a gas chimney [*Løseth et al*., 2009; *Vadakkepuliyambatta et al*., 2013].

Although the interpreted BSRs occur in many basins of the SW Barents Sea, most of them are small and isolated (Figure 2c). This patchy distribution of BSR covers a total area of ~275 km^2. Most of the BSR were located in the Bjørnøyrenna Fault Complex (BFC) and Polheim subplatform close to the Loppa High. Here the largest BSR situated at the western part of Polheim subplatform has a total aerial extent of ~100 km^2. BSR also occur on the Loppa High, Samson Dome, in the Hammerfest Basin, and the Bjørnøya Basin. The interpreted BSR conform with previous BSR observations from the SW Barents Sea [*Andreassen et al*., 1990; *Løvø et al*., 1990; *Laberg and Andreassen*, 1996; *Chand et al*., 2012; *Ostanin et al*., 2013] and expand the seismic evidences of gas hydrate occurrence in this area.

Many of the hydrate-related BSR were associated with gas chimneys that have been identified in this region by *Vadakkepuliyambatta et al*. [2013] (Figure 2c). These gas chimneys could be acting as pathways for the gas that is accumulating in hydrates once it enters the hydrate stability zone. BSRs are also located close to major structural elements such as structural highs and faults, particularly in the BFC area (Figure 2c). Recently, many oil and gas discoveries were made in this region which consists of normal faults, deformed fault planes, and reverse faults. Reactivation of these faults took place during Late Cretaceous and Tertiary [*Riis et al*., 1986], which may have resulted in spillage of hydrocarbons from traps [*Nyland et al*., 1992; *Henriksen et al*., 2011]. The presence of gas chimneys and major structural features close to interpreted BSR emphasizes the importance of gas source and gas composition in the formation of hydrates.

We did not observe seismic evidence for gas hydrate accumulations within the SI methane hydrate stability zone (Figure 2d and Table S5). Relatively shallow depths and high BWTs are the major factors limiting the methane hydrate stability in most parts of the SW Barents Sea. Pure methane hydrates are stable only at a few locations and did not match with interpreted BSR (Figure 2d and Table S5). These observations suggest that pure methane hydrates are not widespread in the SW Barents Sea.

However, it must be stated that bad data quality and lack of coverage may have limited the identification of seismic evidences for hydrates, particularly in the northern part of the study area (Figure S1). Due to these reasons, an even wider occurrence of SI and SII methane hydrates cannot be ruled out.

4.3. Response of GHSZ to Ocean Warming

The response of the thermogenic gas hydrate system in a very dynamic Barents Sea environment is analyzed based on historic data and future projections (Figure 3). For the period 1960–2010, where historic BWTs are

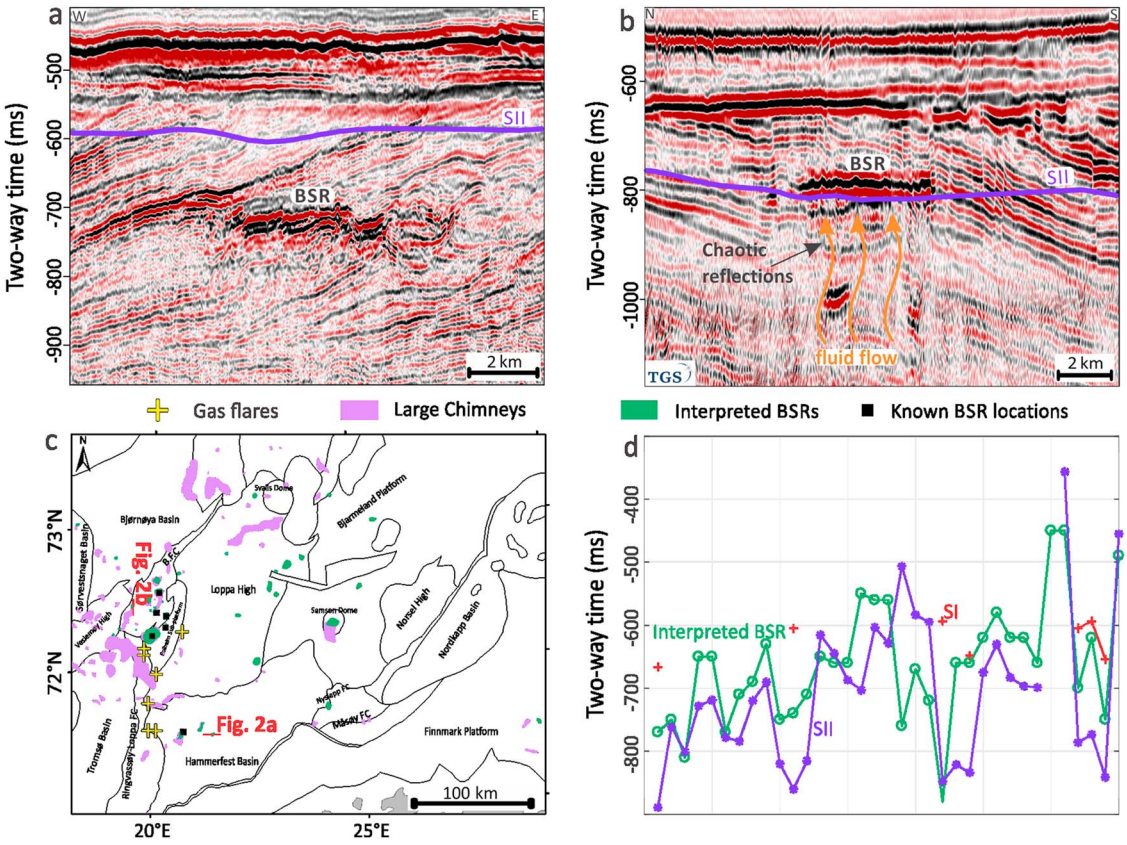

Figure 2. Probable gas hydrate-related BSR in the SW Barents Sea. (a) Seismic profile from the Hammerfest Basin shows gas hydrate-related BSR deeper than the modeled base of GHSZ for SII hydrates. (b) BSR-like reflection from the Bjørnøyrenna Fault Complex (BFC) matching the base of hydrate stability zone for SII hydrates. (c) Distribution of interpreted seismic BSR along with large gas chimneys [*Vadakkepuliyambatta et al*., 2013], location of known gas hydrate accumulations [*Andreassen et al*., 1990; *Løvø et al*., 1990; *Laberg and Andreassen*, 1996; *Chand et al*., 2012; *Ostanin et al*., 2013], gas flare locations [*Chand et al*., 2012], and major structural elements (black lines) (Norwegian Petroleum Directorate Factmaps, http://npdmap1.npd.no/website/NPDGIS/viewer.htm). (d) Comparison between modeled base of GHSZ and interpreted BSR in seismic two-way time. Model for SI hydrates consistently underestimates the depth of BSR all over the SW Barents Sea (unstable at most of interpreted BSR locations) suggesting widespread existence of higher-order hydrocarbons within the GHSZ (Locations of interpreted BSR are shown in Table S5).

used, the GHSZ thicknesses of both SI and SII gas hydrates increased during the first few decades (Figure 3). This is primarily due to the bottom water cooling, which is attributed to El Niño event that occurred during 1982–1983 [*Ferré et al*., 2012]. The GHSZ tends to reduce in thickness until 2060 if all the parameters except the linear increase in BWT are in steady state. The incursion of Atlantic water mass played a major role in the thinning of GHSZ thickness during 1985–2010 period. This is highlighted by the northward migration of cold water front (CWF) (2.5°C BWT contour) (Figure 3).

Due to the relatively slow transport of heat through sediments, increase in BWT will not be able to disturb hydrate stability conditions deeper than ~80 m below the seafloor in the time period we are considering here (Figures 4a and 4b). Although pure methane hydrates (SI) are affected most by the ocean warming, as indicated by the aerial extent of hydrate dissociation, both SI and SII hydrates within the upper 70–80 m of sediments could be at risk of dissociation (Figure 4b). Such top-down hydrate dissociation can occur at shallow water depths (250–350 m) if the temperature variation is significant, as opposed to hydrate dissociation at the base of GHSZ, suggested in West Svalbard margin [*Marín-Moreno et al*., 2013]. In addition, owing to the variability of gas composition (See Supporting Information S2), a much larger region representing GHSZ, which falls between SI and SII gas compositions (grey region, Figure 4a), could be potentially affected by warming bottom waters. Over the period of the modeled years, ongoing ocean bottom temperature warming could potentially result in destabilizing gas hydrates close to the seafloor in a large region covering up to 38% of the SW Barents Sea (Figure 4a), assuming hydrate occurrence at the modeled locations. Considering

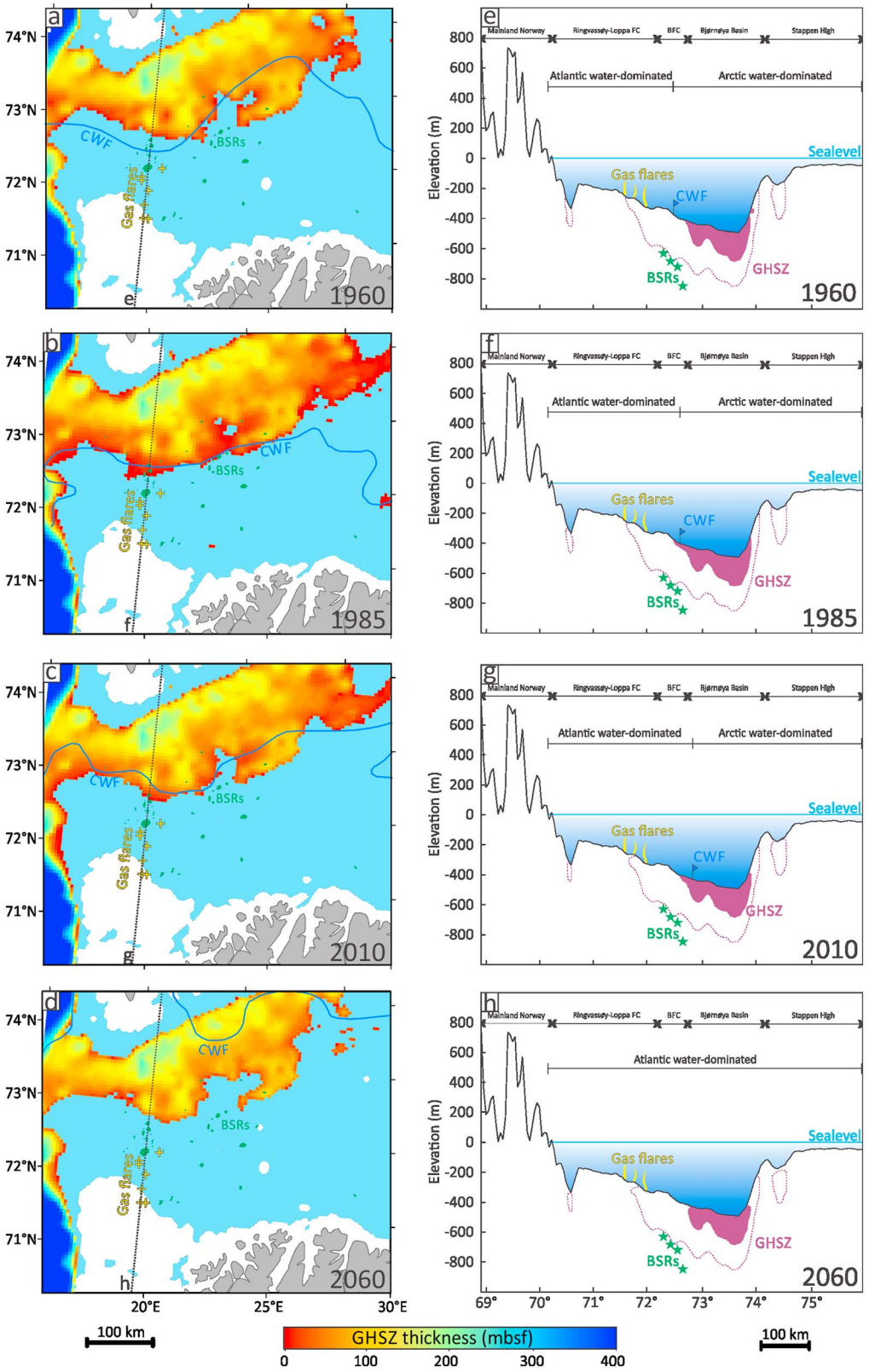

Figure 3. Dynamic changes in GHSZ due to variations in the bottom water temperatures during the period 1960–2010. (a–d) The aerial extent of GHSZ for SI (GHSZ thickness color coded) and SII hydrates (light blue shaded) is shown along with the distribution of seismic BSR and gas flares. CWF represents the cold water front defined as the 2.5°C BWT contour. (e–h) North-south 2-D profiles highlight the vertical changes in the thickness of GHSZ for SI (purple shaded) and SII (purple dashed lines) hydrates. Gas flares, observed BSR, and shifting CWF are also shown. Note the shallow hydrate destabilization by the year 2060.

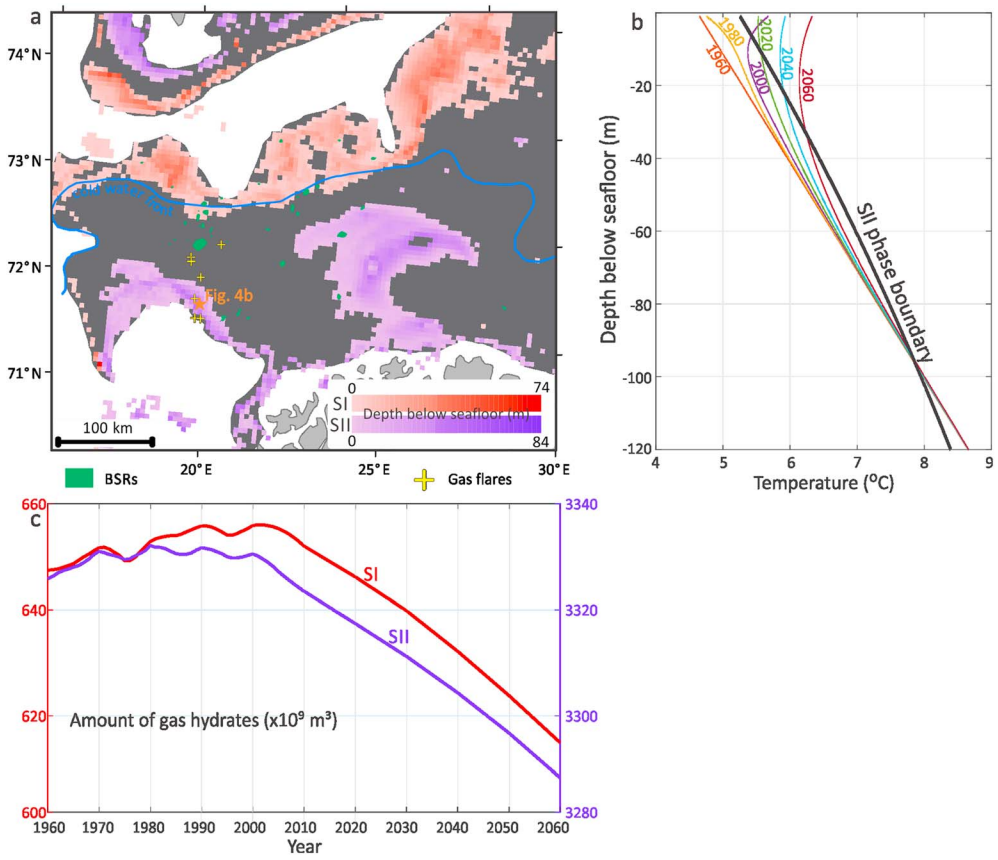

Figure 4. (a) Regions of shallow gas hydrate destabilization as a result of temperature variations during the period 1960–2060. The grey shaded region represents the area of dissociation for hydrates with gas composition between SI and SII (methane content in between 96% and 100%). (b) 1-D temperature propagation through sediments for the period 1960–2060. SII hydrates at the modeled location (Figure 4a) start destabilization from the seafloor by the year 2000. (c) Variation in the amount of gas hydrates trapped within the sediments over the period 1960–2060 for SI and SII hydrates.

only the BSR observed in our seismic data that are within the dissociation region, a negligible fraction of the SW Barents Sea (0.03%) will be prone to hydrate dissociation.

4.4. Implications

The gas seeps recently detected in the SW Barents Sea [*Chand et al.*, 2012] occur close to the area of SII hydrate destabilization (Figures 3 and 4a). Some of these gas seeps also occur in the region where hydrates are supposed to be unaffected by warming ocean waters. The discharge of methane gas into the ocean in these locations could be either due to focused fluid flow (e.g., gas chimneys) transporting the gas all the way up to the seafloor similar to those observed at NW Svalbard [*Hustoft et al.*, 2009], aided by the lack of pure methane hydrate stability conditions, or the result of seasonal BWT variations causing hydrate destabilization (few meters below seafloor) [*Berndt et al.*, 2014].

Based on the modeling, a significant volume of hydrates could be destabilized due to ocean warming in the SW Barents Sea (Figure 4b). Assuming a 7% hydrate saturation in the pore space [*Laberg et al.*, 1998], 40% porosity, and 94% cage occupancy [*Lorenson and Collett*, 2000], up to 93×10^9 m^3 of hydrates could dissociate from SI and SII hydrates during the modeled period (Figure 4b). It represents up to 8 Gt of carbon that could potentially release into the water column. Our estimates provide an upper limit on the amount of hydrate that could be dissociated from the SW Barents Sea using a simplistic scenario without taking into account heat variations due to hydrate formation/dissociation and the transport of free gas through the sedimentary strata [*Stranne et al.*, 2016b, 2016a]. This augments other studies which analyzed response of methane hydrates to warming ocean waters in the Arctic [*Biastoch et al.*, 2011; *Kretschmer et al.*, 2015; *Marín-Moreno*

et al., 2016], Alaskan Beaufort margin [*Phrampus et al*., 2014], West Svalbard [*Marín-Moreno et al*., 2013; *Thatcher et al*., 2013; *Marín-Moreno et al*., 2015], and East Siberian continental slope [*Stranne et al*., 2016b]. Compared to recent estimations of carbon trapped in hydrates in the Arctic, our estimate of hydrate dissociation from the SW Barents Sea could represent up to ~7% of the overall estimate [*Kretschmer et al*., 2015]. It also represents ~15 times the carbon trapped in Vestnesa Ridge [*Hustoft et al*., 2009] and is 3 orders of magnitude higher than the future emission estimate from offshore Svalbard [*Marín-Moreno et al*., 2013]. Compared to present-day active seepage offshore Svalbard [*Sahling et al*., 2014], our estimate is 5 orders of magnitude higher. Most of the above mentioned studies, however, do not consider how thermogenic gas hydrates could be affected by ocean warming, though it can occupy a much larger region both laterally and vertically in the sediments and could potentially store more carbon than pure methane hydrates. This can be particularly important in the Barents Sea as well as Vestnesa Ridge, Beaufort Shelf, and Kara Sea in the Arctic, where petroleum systems are known to exist [*Spencer et al*., 2011; *Dumke et al*., 2016]. The total amount of carbon released during hydrate dissociation is halved if we omit SII hydrates from the hydrate dissociation estimate in the SW Barents Sea.

Most of the observed BSR occur at a depth close to or deeper than the base of GHSZ of SII hydrates (Figures 2 and 3). Assuming that most of the upward migrating gas form hydrates at or above the BSR or get trapped under the BSR and no in situ production of methane, it is likely that the hydrate saturation within the sediments would be significantly low in the shallow sediments [e.g., *Hustoft et al*., 2009]. Thus, it is highly unlikely that significant hydrate dissociation may occur at any of the observed hydrate locations, even though they occur within the area where hydrates are predicted to be destabilized (Figures 3 and 4a). This implies that the models may overestimate the amount of hydrate dissociation due to ocean warming. Based on this assumption, considering very conservative values for hydrate saturation (1%) and porosity (40%), at least $13 \times 10^9\,m^3$ (~1.2 Gt of carbon) of hydrates could be dissociated from dissociation of SI and SII hydrates. Although we could not identify any probable hydrate accumulations within the shallow sediments from the seismic data due to limitations in seismic resolution and due to the difficulties associated with directly inferring gas hydrates seismically above the base of the GHSZ, the potential for occurrence of hydrate accumulations within shallow sediments cannot be ruled out.

5. Conclusions

We provide an integrated analysis of seismic data and transient hydrate stability modeling over the SW Barents Sea during the period 1960–2060, which reveals numerous previously undetected BSR and potential dissociation of hydrate accumulations due to future ocean warming. Most of the observed BSR occur close to the SII GHSZ indicating significant thermogenic gas input into the hydrate stability zone throughout the SW Barents Sea. The distribution of BSR is controlled primarily by focused fluid flow features, such as gas chimneys and faults. A 1°C increase in ocean bottom temperatures over the recent past and future (1960–2060) could result in the dissociation of hydrates present in shallow sediments over 0.03–38% of the SW Barents Sea. Our study predicts that $\sim 13–93 \times 10^9\,m^3$ (1–8 Gt of carbon) of hydrates could dissociate in the SW Barents Sea over the 100 years. The SW Barents Sea makes for an excellent natural laboratory for hydrate dissociation studies as dynamic ocean circulation could affect up to 7% of the total carbon inventory trapped as hydrates in the Arctic.

Acknowledgments

This research is part of the Centre for Arctic Gas Hydrate, Environment and Climate (CAGE) and was supported by the Research Council of Norway through its Centers of Excellence funding scheme grant 223259. Norwegian Petroleum Directorate is acknowledged for providing 2-D seismic and exploration well data through DISKOS data repository. The seismic and well data are available for academic purposes through the Diskos National Data Repository (http://www.diskos.no/). We acknowledge NOAA-NODC for access to the bottom water temperatures (https://www.nodc.noaa.gov/OC5/WOD13/). We thank TGS-NOPEC geophysical company for providing some of the 2-D seismic data. The seismic data can be accessed for academic purposes by contacting TGS (http://www.tgs.com/data-library/). Thanks to Schlumberger for assistance with Petrel interpretation software. We thank Hector Marin-Moreno and an anonymous reviewer for their comments which improved the manuscript.

References

Andreassen, K., K. Hogstad, and K. A. Berteussen (1990), Gas hydrate in the southern Barents Sea, indicated by a shallow seismic anomaly, *First Break*, *8*(6), 235–245.

Berndt, C., et al. (2014), Temporal constraints on hydrate-controlled methane seepage off Svalbard, *Science*, *343*(6168), 284–287.

Biastoch, A., et al. (2011), Rising Arctic Ocean temperatures cause gas hydrate destabilization and ocean acidification, *Geophys. Res. Lett.*, *38*, L08602, doi:10.1029/2011GL047222.

Brady, N. C., and R. R. Weil (1996), *The Nature and Properties of Soils*, 11th ed., Prentice Hall, New York.

Bugge, T., S. Befring, R. Belderson, T. Eidvin, E. Jansen, N. Kenyon, H. Holtedahl, and H. Sejrup (1987), A giant three-stage submarine slide off Norway, *Geo Mar. Lett.*, *7*(4), 191–198.

Bugge, T., G. Elvebakk, S. Fanavoll, G. Mangerud, M. Smelror, H. M. Weiss, J. Gjelberg, S. E. Kristensen, and K. Nilsen (2002), Shallow stratigraphic drilling applied in hydrocarbon exploration of the Nordkapp Basin, Barents Sea, *Mar. Pet. Geol.*, *19*(1), 13–37.

Cavanagh, A. J., R. Di Primio, M. Scheck-Wenderoth, and B. Horsfield (2006), Severity and timing of Cenozoic exhumation in the southwestern Barents Sea, *J. Geol. Soc.*, *163*(5), 761–774.

Chand, S., J. Mienert, K. Andreassen, J. Knies, L. Plassen, and B. Fotland (2008), Gas hydrate stability zone modelling in areas of salt tectonics and pockmarks of the Barents Sea suggests an active hydrocarbon venting system, *Mar. Pet. Geol.*, *25*, 625–636.

Chand, S., T. Thorsnes, L. Rise, H. Brunstad, D. Stoddart, R. Bøe, P. Lågstad, and T. Svolsbru (2012), Multiple episodes of fluid flow in the SW Barents Sea (Loppa High) evidenced by gas flares, pockmarks and gas hydrate accumulation, *Earth Planet. Sci. Lett.*, *331–332*, 305–314.
Doré, A. G., and L. N. Jensen (1996), The impact of late Cenozoic uplift and erosion on hydrocarbon exploration: Offshore Norway and some other uplifted basins, *Global Planet. Change*, *12*(1-4), 415–436.
Dumke, I., E. B. Burwicz, C. Berndt, D. Klaeschen, T. Feseker, W. H. Geissler, and S. Sarkar (2016), Gas hydrate distribution and hydrocarbon maturation north of the Knipovich Ridge, western Svalbard margin, *J. Geophys. Res. Solid Earth*, *121*, 1405–1424, doi:10.1002/2015JB012083.
Duran, E. R., R. di Primio, Z. Anka, D. Stoddart, and B. Horsfield (2013), 3D-basin modelling of the Hammerfest Basin (southwestern Barents Sea): A quantitative assessment of petroleum generation, migration and leakage, *Mar. Pet. Geol.*, *45*, 281–303.
Ferré, B., J. Mienert, and T. Feseker (2012), Ocean temperature variability for the past 60 years on the Norwegian-Svalbard margin influences gas hydrate stability on human time scales, *J. Geophys. Res.*, *117*, C10017, doi:10.1029/2012JC008300.
Fetterer, F., K. Knowles, W. Meier, and M. Savoie (2016), *Sea Ice Index Version 2*, Natl. Snow and Ice Data Cent., Boulder, Colo.
Gerya, T. (2010), *Introduction to Numerical Geodynamic Modeling*, Cambridge Univ. Press, Cambridge, U. K.
Henriksen, E., et al. (2011), Chapter 17 Uplift and erosion of the greater Barents Sea: Impact on prospectivity and petroleum systems, *Geol. Soc. Lond. Mem.*, *35*(1), 271–281.
Hustoft, S., S. Bünz, J. Mienert, and S. Chand (2009), Gas hydrate reservoir and active methane-venting province in sediments on <20 Ma young oceanic crust in the Fram Strait, offshore NW-Svalbard, *Earth Planet. Sci. Lett.*, *284*(1–2), 12–24.
Jakobsson, M., et al. (2012), The International Bathymetric Chart of the Arctic Ocean (IBCAO) version 3.0, *Geophys. Res. Lett.*, *39*, L12609, doi:10.1029/2012GL052219.
Kennett, J. P., K. G. Cannariato, I. L. Hendy, and R. J. Behl (2003), *Methane Hydrates in Quaternary Climate Change—The Clathrate Gun Hypothesis*, AGU, Washington, D. C.
Kretschmer, K., A. Biastoch, L. Rüpke, and E. Burwicz (2015), Modeling the fate of methane hydrates under global warming, *Global Biogeochem. Cycles*, *29*, 610–625, doi:10.1002/2014GB005011.
Kvenvolden, K. A. (1988), Methane hydrate—A major reservoir of carbon in the shallow geosphere?, *Chem. Geol.*, *71*(1–3), 41–51.
Kvenvolden, K. A., and M. A. McMenamin (1980), Hydrates of natural gas: A review of their geologic occurrence, *U.S. Geol. Surv. Circular*, *No. 825*, 11.
Laberg, J. S., and K. Andreassen (1996), Gas hydrate and free gas indications within the Cenozoic succession of the Bjornoya Basin, western Barents Sea, *Mar. Pet. Geol.*, *13*(8), 921–940.
Laberg, J. S., K. Andreassen, and S. M. Knutsen (1998), Inferred gas hydrate on the Barents Sea shelf—A model for its formation and a volume estimate, *Geo Mar. Lett.*, *18*(1), 26–33.
Lorenson, T. D., and T. Collett (2000), Gas content and composition of gas hydrate from sediments of the southeastern North American continental margin, in *Proceedings of the Ocean Drilling Program, Scientific Results*, edited by C. K. Paull et al., Ocean Drilling Program, College Station, Tex.
Løseth, H., M. Gading, and L. Wensaas (2009), Hydrocarbon leakage interpreted on seismic data, *Mar. Pet. Geol.*, *26*(7), 1304–1319.
Løvø, V., A. Elverhøi, P. Antonsen, A. Solheim, G. Butenko, O. Gregersen, and O. Liestøl (1990), Submarine permafrost and gas hydrates in the northern Barents Sea, *Norsk Polar Inst. Rapportserie*, *56*, 171.
Marín-Moreno, H., T. A. Minshull, G. K. Westbrook, B. Sinha, and S. Sarkar (2013), The response of methane hydrate beneath the seabed offshore Svalbard to ocean warming during the next three centuries, *Geophys. Res. Lett.*, *40*, 5159–5163, doi:10.1002/grl.50985.
Marín-Moreno, H., T. A. Minshull, G. K. Westbrook, and B. Sinha (2015), Estimates of future warming-induced methane emissions from hydrate offshore west Svalbard for a range of climate models, *Geochem. Geophys. Geosyst.*, *16*, 1307–1323, doi:10.1002/2015GC005737.
Marín-Moreno, H., M. Giustiniani, U. Tinivella, and E. Piñero (2016), The challenges of quantifying the carbon stored in Arctic marine gas hydrate, *Mar. Pet. Geol.*, *71*, 76–82.
Maslin, M., M. Owen, R. Betts, S. Day, T. Dunkley Jones, and A. Ridgwell (2010), Gas hydrates: Past and future geohazard?, *Philos. Trans. R. Soc. A*, *368*(1919), 2369–2393.
National Oceanographic Data Center (NODC) (2013), World Ocean Database. [Available at http://www.nodc.noaa.gov/General/temperature.html, edited.]
Nyland, B., L. N. Jensen, J. Skagen, O. Skarpnes, and T. O. Vorren (1992), Tertiary uplift and erosion in the Barents Sea: Magnitude, timing and consequences, in *Structural and Tectonic Modeling and Its Application to Petroleum Geology (NPF Special Publications 1)*, edited by R. M. Larsen et al., pp. 153–162, Elsevier, Amsterdam.
Ostanin, I., Z. Anka, R. di Primio, and A. Bernal (2012), Identification of a large Upper Cretaceous polygonal fault network in the Hammerfest basin: Implications on the reactivation of regional faulting and gas leakage dynamics, SW Barents Sea, *Mar. Geol.*, *332–334*, 109–125.
Ostanin, I., Z. Anka, R. di Primio, and A. Bernal (2013), Hydrocarbon plumbing systems above the Snøhvit gas field: Structural control and implications for thermogenic methane leakage in the Hammerfest Basin, SW Barents Sea, *Mar. Pet. Geol.*, *43*, 127–146.
Pascal, C. (2015), Heat flow of Norway and its continental shelf, *Mar. Pet. Geol.*, *66*(Part 4), 956–969.
Peters, K. E., and P. H. Nelson (2009), Criteria to determine borehole formation temperatures for calibration of basin and petroleum system models, in *AAPG Annual Convention and Exhibition*, edited by N. B. Harris and K. E. Peters, U.S. Geol. Surv., Denver, Colo.
Phrampus, B. J., and M. J. Hornbach (2012), Recent changes to the Gulf Stream causing widespread gas hydrate destabilization, *Nature*, *490*(7421), 527–530.
Phrampus, B. J., M. J. Hornbach, C. D. Ruppel, and P. E. Hart (2014), Widespread gas hydrate instability on the upper U.S. Beaufort margin, *J. Geophys. Res. Solid Earth*, *119*, 8594–8609, doi:10.1002/2014JB011290.
Riis, F., J. Vollset, and M. Sand (1986), Tectonic development of the western margin of the Barents Sea and adjacent areas, in *Future Petroleum Provinces of the World*, edited by M. T. Halbouty, pp. 661–676, AAPG Memoirs, Tulsa, Okla.
Sahling, H., et al. (2014), Gas emissions at the continental margin west of Svalbard: Mapping, sampling, and quantification, *Biogeosciences*, *11*(21), 6029–6046.
Shipley, T. H., M. H. Houston, R. T. Buffler, F. J. Shaub, K. J. McMillen, J. W. Ladd, and J. L. Worze (1979), Seismic evidence for widespread possible gas hydrate horizons on continental slopes and rises, *AAPG Bull.*, *63*(12), 2204–2213.
Sloan, E. D. (1990), *Clathrate Hydrates of Natural Gases*, Marcel Dekker, New York.
Sloan, E. D., and C. A. Koh (2008), *Clathrate Hydrates of Natural Gases*, 3rd ed., pp. 752, CRC Press, Boca Raton, Fla.
Spencer, A. M., A. F. Embry, D. L. Gautier, A. V. Stoupakova, and K. Sørensen (2011), An overview of the petroleum geology of the Arctic, *Geol. Soc. Lond. Mem.*, *35*(1), 1–15.
Spiegelman, M. (2004), Myths and methods in modeling, in *Columbia University Lecture Notes*. [Available at http://www.ldeo.columbia.edu/~mspieg/mmm/.]

Stranne, C., M. O'Regan, and M. Jakobsson (2016a), Overestimating climate warming-induced methane gas escape from the seafloor by neglecting multiphase flow dynamics, *Geophys. Res. Lett.*, *43*, 8703–8712, doi:10.1002/2016GL070049.

Stranne, C., M. O'Regan, G. R. Dickens, P. Crill, C. Miller, P. Preto, and M. Jakobsson (2016b), Dynamic simulations of potential methane release from East Siberian continental slope sediments, *Geochem. Geophys. Geosyst.*, *17*, 872–886, doi:10.1002/2015GC006119.

Thatcher, K. E., G. K. Westbrook, S. Sarkar, and T. A. Minshull (2013), Methane release from warming-induced hydrate dissociation in the West Svalbard continental margin: Timing, rates, and geological controls, *J. Geophys. Res. Solid Earth*, *118*, 22–38, doi:10.1029/2012JB009605.

Turcotte, D. L., and G. Schubert (2002), *Geodynamics*, Cambridge Univ. Press, New York.

Vadakkepuliyambatta, S., S. Bünz, J. Mienert, and S. Chand (2013), Distribution of subsurface fluid-flow systems in the SW Barents Sea, *Mar. Pet. Geol.*, *43*, 208–221.

Waples, D. W., and J. S. Waples (2004), A review and evaluation of specific heat capacities of rocks, minerals, and subsurface fluids. Part 2: Fluids and porous rocks, *Nat. Resour. Res.*, *13*(2), 123–130.

Westbrook, G. K., et al. (2009), Escape of methane gas from the seabed along the West Spitsbergen continental margin, *Geophys. Res. Lett.*, *36*, L15608, doi:10.1029/2009GL039191.

Woodside, W., and J. H. Messmer (1961), Thermal conductivity of porous media. I. Unconsolidated sands, *J. Appl. Phys.*, *32*(9), 1688–1699.